

HEADREST OR HORSE BIT VFIG 2003.7 – LEADED BRONZE – MODERN TIMES

Artefact name Headrest or horse bit VFig 2003.7

Authors Barbezat. Nadège (HE-Arc CR, Neuchâtel, Neuchâtel, Switzerland) & Christian. Degrigny (HE-Arc CR, Neuchâtel, Neuchâtel, Switzerland) & Valentin. Boissonnas (HE-Arc CR, Neuchâtel, Neuchâtel, Switzerland)

Url /artefacts/961/

▼ The object



Credit HE-Arc CR, N. Barbezat.



Fig. 1: Headrest or horse bit, side and front view,

▼ Description and visual observation

Description of the artefact

The artefact is made of two figurative (winged wild sheep) plates attached by a central bar (Fig. 1). One of the volutes of the bar is filled with metal suggesting it was cast with its end rolled up already. The surfaces of the plates (both sides) and the central bar are covered with a black adherent layer. A heterogeneous green layer is visible over this black layer. Well adhering hard brown-grey sediment-like deposits are present mostly in the middle of the plates on both sides. Red and orange spots are unevenly distributed on the surface (white arrow). Dimensions: W plates = 13mm; H plates = 105mm, L bar = 185mm, WT = 925g.

Type of artefact Headrest or horse bit

Origin Luristan (?)

Recovering date Unknown

Chronology category Modern Times

chronology tpq ----

chronology tag

Chronology comment

20th century (fake)

Burial conditions / environment

Unknown

Artefact location

Bible & Orient Museum, Fribourg, Fribourg

Owner

Bible & Orient Museum, Fribourg, Fribourg

Inv. number

VFig 2003.7

Recorded conservation data

N/A

Complementary information

None.

▼ Study area(s)

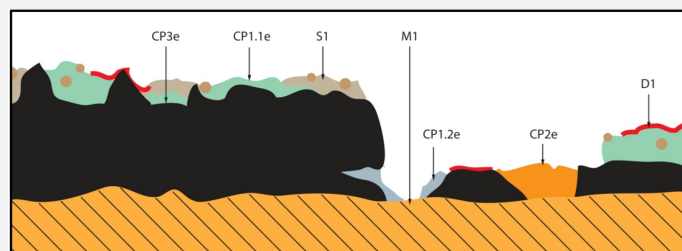


Credit HE-Arc CR, N.Barbezat.

Fig. 2: Location of sampling areas,

▼ Binocular observation and representation of the corrosion structure

The schematic representation below gives an overview of the corrosion layers encountered on the object from visual macroscopic observation (additional e and i within the coding correspond to strata in contact with the environment (e) and internal strata (i)).



S1: soil (sand and limestone)

D1: red deposit

CP1.1e: outer light green-blue corrosion layer

CP1.2e: outer white-blue-grey corrosion layer

CP2e: outer orange corrosion layer

CP3e/i: outer/inner black brown corrosion layer

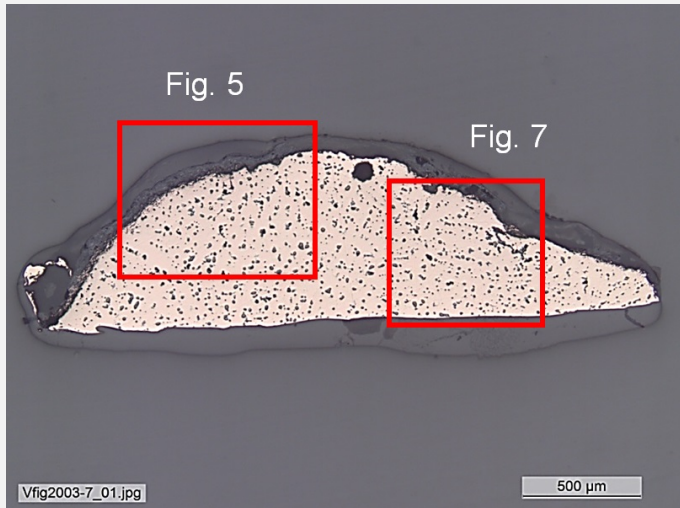
M1: metal

Credit HE-Arc CR, N.Barbezat.

Fig. 3: Stratigraphic representation of the artefact by macroscopic observation,

▽ MiCorr stratigraphy(ies) – Bi

▽ Sample(s)



Credit HE-Arc CR.

Description of sample

The sample was cut on the bottom of one of the plates (Fig. 2). On Fig. 4, the top and round shape of the sample is the outer part of the metal. It is covered with corrosion layers. The lower part of the sample corresponds to the cut metal with no corrosion products.

Alloy

Leaded Bronze

Technology

Cast and cold worked (with final annealing?)

Lab number of sample

None

Sample location

HE-Arc CR, Neuchâtel, Neuchâtel

Responsible institution

Bible & Orient Museum, Fribourg, Fribourg

Date and aim of sampling

2014, metallography and chemical analyses

Complementary information

None.

▽ **Analyses and results**

Analyses performed:

Metallography (etched with ferric chloride reagent), SEM/EDS and FTIR.

❖ Non invasive analysis

None.

❖ Metal

The remaining metal is a leaded bronze (Table 1) containing numerous copper sulphide and lead (Pb) inclusions (Figs. 5 and 6). The porosity is difficult to distinguish since the pores seem to have similar dimensions as the inclusions that could have been removed during the polishing of the sample (Fig. 5). After etching, the structure of the metal appears to be made up mostly of dendrites, but a grain structure seems to have developed on the right side of the sample, with occasional twin lines (Figs. 7 and 8). The twinned grain structure could be the result of cold work and annealing after casting, possibly through the application of an artificial patina under heat.

Elements	Cu	Sn	Pb
mass%	85	7	5

Table 1: Chemical composition of the metal. Method of analysis: SEM-EDS, Lab of Electronic Microscopy and Microanalysis, IMA (Néode), HEI Arc.

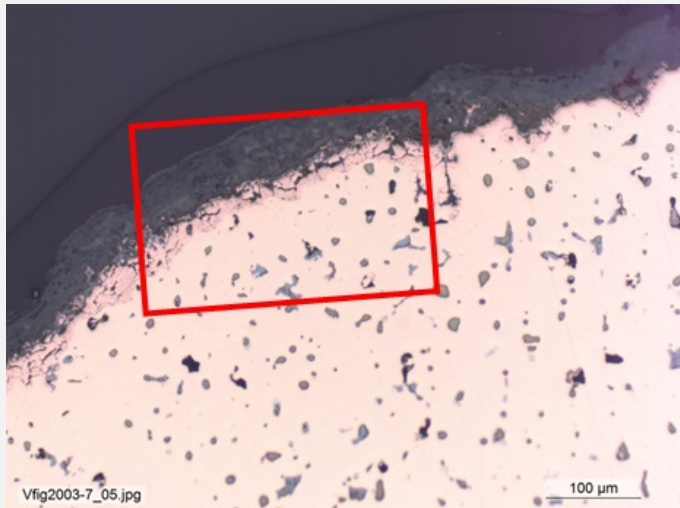


Fig. 5: Micrograph of the cross-section of sample from Fig. 2 of the headrest (or horse bit) (detail of Fig. 4), unetched, bright field. Light grey copper sulphide and tiny round Pb inclusions as well as "porosities" can be observed. Area of Fig. 9 is marked by a red rectangle,

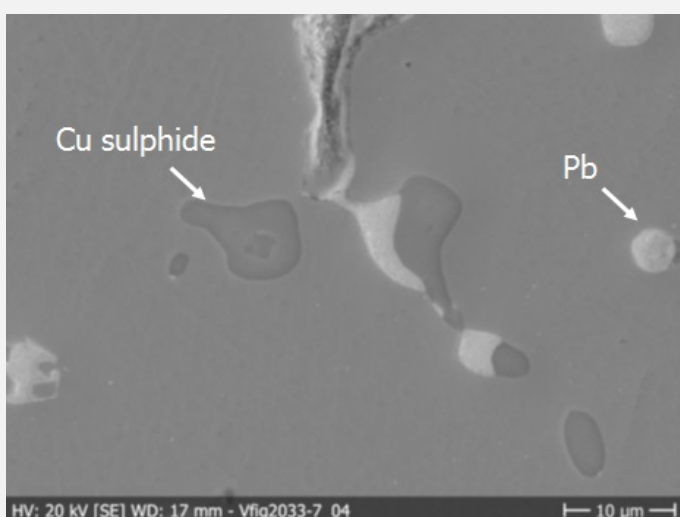


Fig. 6: SEM image (detail of Fig. 5), SE-mode, showing copper sulphide and lead inclusions,



Fig. 7: Micrograph of the metal sample from Fig. 4 showing a dendritic structure and grains,

Credit HE-Arc CR.

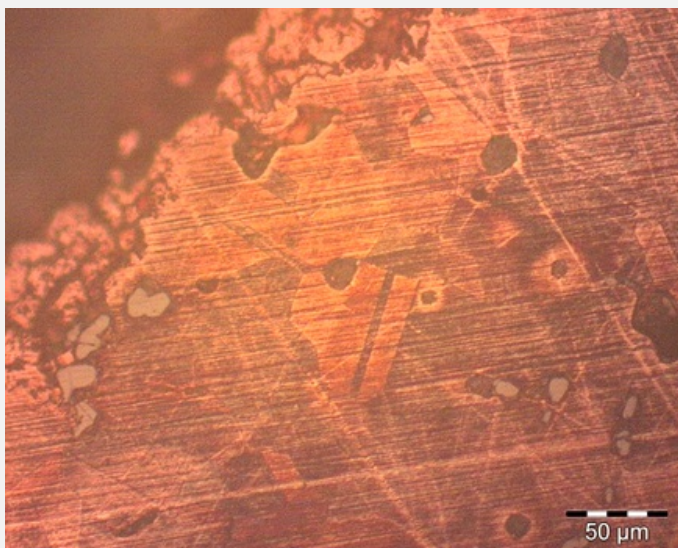


Fig. 8: Micrograph of a selected area of the metal sample showing grains and twin lines,

Credit HE-Arc CR.

Microstructure Dendritic structure & limited grain structure (with twin lines)

First metal element Cu

Other metal elements Sn, Pb

Complementary information

None.

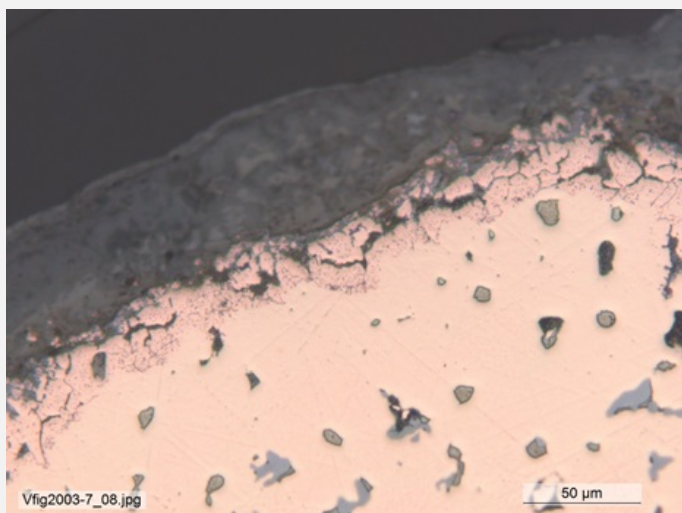
▼ Corrosion layers

The remaining metal seems to have developed intergranular corrosion at the interface metal / corrosion layer (Fig. 9) slightly enriched in Sn (Fig. 11). The outer green corrosion product (CP2) is matte, powdery and mixed with sediments. It looks regular on Figs. 9 and 10 (around 50µm). This corrosion layer is mainly composed of lead (and/or sulphur), oxygen, silicon, chlorine and is depleted in Cu (Fig. 11 and table 2) except in its top part (CP1) where it is Cl, Cu and O-rich (Fig. 11 and table 2). FTIR seems to indicate that it is constituted of atacamite ($\text{Cu}_2\text{Cl}(\text{OH})_3$, Fig. 12). This is confirmed on the EDS spectra of figure 13 where Pb is clearly detected. The inner corrosion product (CP3) is a dark

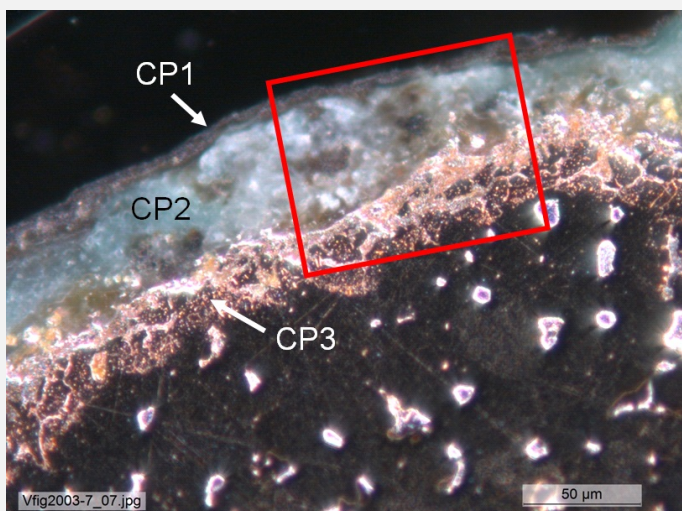
brown, matte layer (Figs. 2 and 10). It covers all the surface of the object, and forms a very thin layer. It is sulphur and oxygen-rich (Fig. 14). FTIR analysis could not reveal the presence of a specific corrosion product.

Elements proportions	O	Si	Cl	Pb/S	Cu	Sn
Blue corrosion product (CP1)	++	(+)	+	++	+	nd
Green corrosion product (CP2)	+	++	(+)	++	(+)	nd
Remnant metal phase	nd	nd	nd	+	++	++

Table 2: Chemical composition of the corrosion crust from Fig. 10. Method of analysis: SEM-EDS, Lab of Electronic Microscopy and Microanalysis, IMA (Néode), HEI Arc (+++: high concentration, ++ medium concentration, + low concentration, nd: not-detected).



Credit HE-Arc CR.



Credit HE-Arc CR.

Fig. 9: Micrograph of the metal sample from Fig. 5, unetched, bright field,

Fig. 10: Micrograph similar to Fig. 9 and corresponding to the stratigraphy of Fig. 15, polarised light. The area selected for elemental chemical distribution (Fig. 11) is marked by a red rectangle,

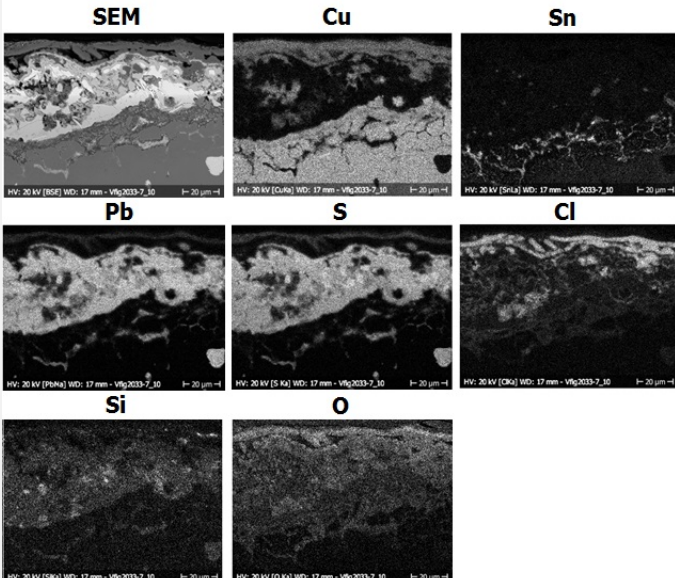


Fig. 11: SEM image, SE-mode, and elemental chemical distribution of the selected area of Fig. 10. Method of examination: SEM-EDS, Lab of Electronic Microscopy and Microanalysis, IMA (Néode), HEI Arc,

Credit HEI Arc, S.Ramseyer.

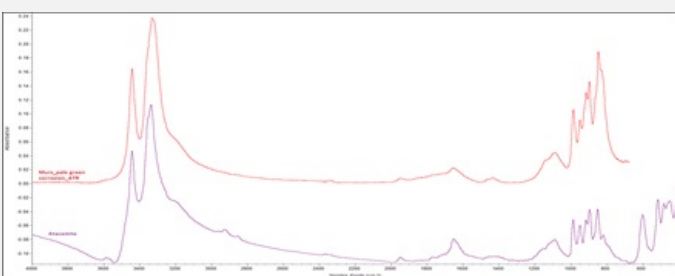


Fig. 12: FTIR spectrum (ATR mode) of the green corrosion powder and comparison to atacamite (purple) spectrum. Method of analysis: FTIR spectroscopy, HE- Arc CR,

Credit HE-Arc CR.

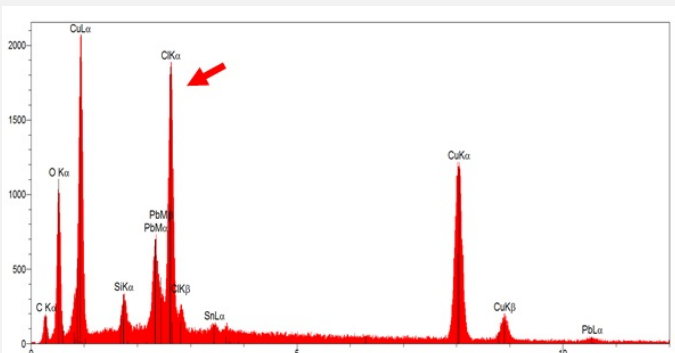


Fig. 13: EDS analysis of the green corrosion powder (Fig. 2). Method of analysis: SEM-EDS, Lab of Electronic Microscopy and Microanalysis, IMA (Néode), HEI Arc,

Credit HE-Arc CR.

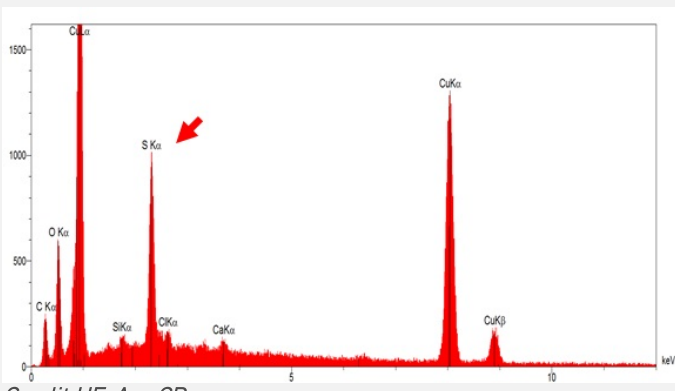


Fig. 14: EDS analysis of the black corrosion powder (Fig. 2). Method of analysis: SEM-EDS, Lab of Electronic Microscopy and Microanalysis, IMA (Néode), HEI Arc,

Corrosion form Uniform - intergranular

Corrosion type Artificial

Complementary information

None.

❖ MiCorr stratigraphy(ies) – CS

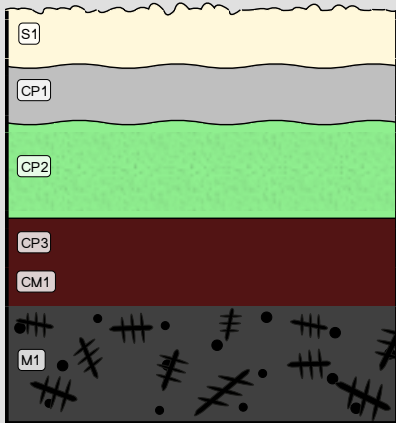


Fig. 15: Stratigraphic representation of sample from Fig. 2 of the headrest (or horse bit) in cross-section (dark field) using the MiCorr application. The characteristics of the strata are only accessible by clicking on the drawing that redirects you to the search tool by stratigraphy representation. This representation can be compared to Fig 10, Credit HE-Arc CR.

❖ Synthesis of the binocular / cross-section examination of the corrosion structure

The schematic representation of corrosion layers of Fig. 3 integrating additional information based on the analyses carried out is given in Fig. 16. A thin, black sulphur-rich layer covers the metal surface. A thick green layer has developed on top and seems to be constituted mainly of atacamite enriched in lead with sediments on top.

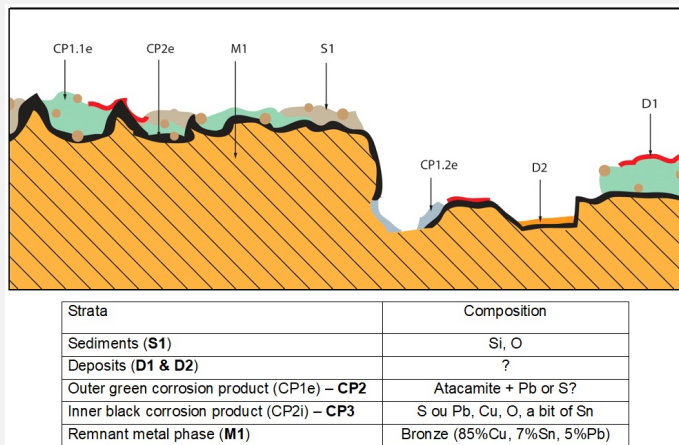


Fig. 16: Improved stratigraphic representation of the headrest from visual observations and analyses (additional mention e or i within the coding correspond to strata in contact with the environment (e) and internal strata (i),

Credit HE-Arc CR, N.Barbezat.

❖ Conclusion

The artefact is a cast leaded bronze that has been partially annealed after cold working (surface finishing?). Strangely enough, one of the rolled up ends of the middle bar is filled with metal, testifying that it was cast already rolled-up. Normally it would have been rolled up after inserting the plates. The remaining metal seems to have developed intergranular corrosion limited to the interface metal / corrosion layers. The corrosion crust is constituted of an outer thick, green atacamite layer enriched in Pb and mixed with sediments while the inner thin, dark brown corrosion layer is S, Cu and O-rich. This stratigraphy is unexpected for an archaeological artefact where we would

expect chlorine to be at the interface metal / corrosion layer. Similarly, Si should be located on top layers although it was found deep in the outer green layer. Furthermore, S is found next to the metal surface while it should be present in higher concentrations in the top layers. Finally, Sn appears in an irregular and interrupted layer on top of the remaining metal. In an archaeological bronze it should be found as a clearly defined enriched layer. The red spots that looked like cuprite turned out to be paint. Since chlorine and sulphur are commonly used for the artificial patination of bronzes, we tend to conclude that this object is probably a fake produced during the 20th century.

▼ References

References on object and sample

Reference object

1. Houshang, M. (1997) Art of ancient Iran: Copper and Bronze. Philip Wilson, London.
2. Rickenbach, J. (1992) Magier mit Feuer und Erz. Museum Rietberg, Zürich, 1992.

References on analytic methods and interpretation

3. Craddock, P. (2009) Scientific investigation of copies, fakes and forgeries. Butterworth-Heinemann, Oxford.
4. Northover, P. (1997) "Appendix". In Houshang Mahboubian. Art of ancient Iran: Copper and Bronze. Philip Wilson, London, 325-338.
5. Oudbashi, O. and al. (2013) Micro-stratigraphical investigation on corrosion layers in ancient Bronze artefacts by scanning electron microscopy energy dispersive spectrometry and optical microscopy. Heritage Science, 1, 21.
6. Oudbashi, O. and al. (2014) Bronze in Archaeology: A Review of the Archaeometallurgy of Bronze in Ancient Iran". In INTECH [Online]. 2012 [consulted on february, the 21th 2014]. <http://www.intechopen.com/books/copper-alloys-early-applications-and-current-performance-enhancing-processes/bronze-in-archaeology-a-review-on-archaeometallurgy-of-bronze-in-ancient-iran>